Nano World Journal

https://doi.org/10.17756/nwj.2023-s1-034

Research Article

Open Access

Numerical Assessment of Hybrid Laser-arc Welding of NV E690 Steel

Alok Kumar, Umesh Kumar Singh*, Avanish Kumar Dubey and Pratiksha

Mechanical Engineering Department, MNNIT Allahabad, Prayagraj, Uttar Pradesh, India

***Correspondence to:**
Umesh Kumar Singh
Mechanical Engineering Department,
MNNIT Allahabad, Prayagraj,
Uttar Pradesh, India.
E-mail: umeshkumarsingh2008@gmail.com

Received: November 24, 2022
Accepted: April 07, 2023
Published: April 09, 2023

Citation: Alok K, Umesh KS, Avanish KD, Pratiksha. 2023. Numerical Assessment of Hybrid Laser-arc Welding of NV E690 Steel. *NanoWorld J* 9(S1): S166-S170.

Published by United Scientific Group

Abstract

NV E690 is a recently developed martensitic steel and shows excellent strength and is used in manufacturing of offshore platforms. The conventional fusion welding methods are unable to meet the industrial demands related to weld quality, but the hybrid laser-arc welding (HLAW) has this capability. The present work demonstrates the numerical investigation of HLAW of 2.0 mm NV E690 steel to predict influence of welding variables on process temperature and thermal stresses in the weldment. In this work, a three-dimensional (3-D) thermo-mechanically based finite element model (FEM) is utilized using ANSYS software for all numerical investigations. The outcome of present research shows that thermal gradient and stresses may suitably be controlled by controlling the laser power (LP), arc voltage, arc current and welding speed (WS). The process peak temperature decreases with increase in WS while it has increasing nature with increase in LP and arc power, separately. But the normal stresses have decreasing nature with increase in LP and arc power, separately.

Keywords

Laser, Arc welding, NV E690 steel, Temperature, Stresses, Welding

Introduction

Automobile, marine engineering and aerospace industries require light weight and high strength materials therefore these industries recommend the high strength low alloy steels. NV E690 is a recently developed martensitic steel which has economic advantages because of lower consumption of alloying elements and poses excellent mechanical properties [1]. Since automobile, marine engineering and aerospace industries demand both high weld quality and efficiency. The gas-metal-arc-welding (GMAW) and tungsten-inert-gas welding are the conventional fusion welding techniques and are not able to meet the today's progressive demands of modern manufacturing industries with respect to quality of the welded products. To overcome this difficulty, laser welding was adopted but with respect to time new advanced materials are developed and laser welding of these material again creates problem due to high thermal conductivity and reflectivity of materials and formation of porosity in deep penetration. HLAW when compared with arc welding and laser welding, has been gaining significant recognition due to its nature of deep penetration, high weld speed, wider gap-bridging capability, excellent appearance of welded surface and weld quality and its higher welding efficiency [1, 2].

Welding induced residual stress is the major concerned problem in welded structures. Therefore, it becomes the matter of research to access the developed residual stresses during the welding process. These stresses not only affect the performance of structure but also the mechanical properties of weldments. A lot of numerical studies were conducted to simulate the hybrid welding process in

view of process characteristics. Sun et al. investigated the thermal profile and residual stresses in laser-MIG hybrid welding of NV E690 steel plates and the study result showed that a considerable amount of tensile longitudinal stresses was developed at and nearby area of the fusion zone (FZ) but the magnitudes of these stresses in heat affected zone were somewhat higher than that in FZ [3]. Yazdian et al. introduced numerical model to simulate the HLAW of 8 mm thick HSQTS using SYSWELD for prediction of distortion and residual stresses in the weldment. The numerical results show good agreement with experimental results. The profile of residual stresses was noticeable due to the tensile residual stresses at the FZ and its nearby area. But overall longitudinal and transverse residual stresses induced by the phase transformation may have led to the depletion of the tensile residual stresses [4]. Xu et al. proposed a model for residual stresses and deformations induced in HLAW of 12-mm-thickness Q460 steel plates. They concluded that the higher longitudinal stress which was tensile in nature, was located at FZ and its nearby area with its maximum value higher than the yield stress of parent material [5]. To obtain the best welding method in purpose of reducing the welding difficulty of invar 36 alloy, Zhan et al. compared the hybrid laser-MIG welding and MIG welding. They observed that the total welding time, material consumption and deformation in MIG welding was 8-times, 4-times, and 3-times, respectively higher than the hybrid laser-MIG welding. This was due to the reason of increasing the weld layers and welding passes in MIG welding [6]. Derakhshan et al. compared the results of different welding methods for evaluation of residual stresses and distortion in welding of 4mm thick A1011-50 steel by experimentally and numerically (SYSWELD). The used welding methods are either laser-based welding or submerged arc welding. They observed that the application of the laser when combined with arc welding significantly reduces the level of residual stresses in weldments as compared to submerged arc welding [7]. Kong et al. used experimental and numerical approach to calculate the residual stresses in HLGMAW of 6 mm thick steel. They observed that the increase in WS lowers the concentration of residual stresses in weldment [8].

The available literature suggests that different laser-based hybrid fusion welding methods were adopted for welding of different grades of steels to access the weldment characteristics. The objective of present research work is focused on numerical assessment of HLAW of NV E690 steel to predict the thermal gradient and thermal stresses in the weldment which are the major drawbacks of welding process. For this work, a 2.0 mm thick sheet of NV E690 steel has been taken as workpiece material and laser power (LP), arc power and WS as process parameters. Simulation work is performed by using finite element based ANSYS APDL software.

Materials and Methods

Material

The material considered in this work was NV E690 steel having 2.0 mm thickness 20 mm length and 16 mm width. The major alloying compositions, thermo-physical and thermo-mechanical properties of material are listed in Table 1, table 2, and table 3, respectively.

Table 1: Alloying compositions of NV E690 steel.

C	0.138
Si	0.28
Mn	1.28
P	0.0185
Ti	0.0068
V	0.0032
Cu	0.014
Al	0.0281
S	0.0052
Ni	0.011
Cr	0.176
Mo	0.119

Table 2: Thermo-physical (temperature dependent) properties of NV E690 steel.

Temp (°C)	20	100	500	780	1200	1500
ρ (kg/m^3)	7820	7700	7610	7550	7490	7350
C (J/kg/°C)	460	710	960	650	690	700
K (W/m/°C)	60	58	39	20	32	35

Table 3: Thermo-mechanical (temperature dependent) properties of NV E690 steel.

Temp (°C)	20	100	500	780	1200	1500
E (GPa)	210	205	130	40	20	20
PR	0.28	0.29	0.30	0.32	0.35	0.41
TEC (10^{-7}°C)	125	130	150	140	170	220

Where, symbols ρ, C, K, E, PR and TEC represents density, specific heat, conductivity, young's modulus, Poisson's ratio and thermal expansion coefficient of material, respectively.

Finite element modeling

Finite element based ANSYS APDL software is used to create FEM to access the thermal gradient and residual stresses in the weldment. Graphical user interface was implemented to create the model, applying temperature dependent thermo-physical and thermo-mechanical properties of material, meshing the work domain, and applying initial and boundary conditions, convection, and heat flux. First, the temperature history and its distribution were computed and then the temperature histories obtained through thermal analysis were imported as thermal loads for mechanical analysis. The following assumptions were made to develop the FEM based model:

- The initial temperature of the work piece surface was taken as 27 °C (300 K).
- The moving heat source was considered while keeping the workpiece fixed in the space.
- Convective heat transfer was applied on all the surfaces except vertical surfaces to be joined.

Material was considered as isotropic and homogenous.

Geometry and mesh

The SOLID70, which has 8 nodes with only temperature

as a degree of freedom at each node has been used in thermal analysis. For mechanical analysis, SOLID185 element (8 nodes and three degree of freedom) was used because it has plasticity, stress, stiffening, large deflection, and large strain capabilities [9]. Tetrahedral mesh was used for whole the region of the workpiece. Fine and same size mesh for the workpiece takes a lot of time to simulate but it gives better result as compared to those models in which coarse, different mesh size and different elements are taken in different region of workpiece. But in present work, for optimized performance of computing system, variable size of mesh was adopted [10] as shown in figure 1.

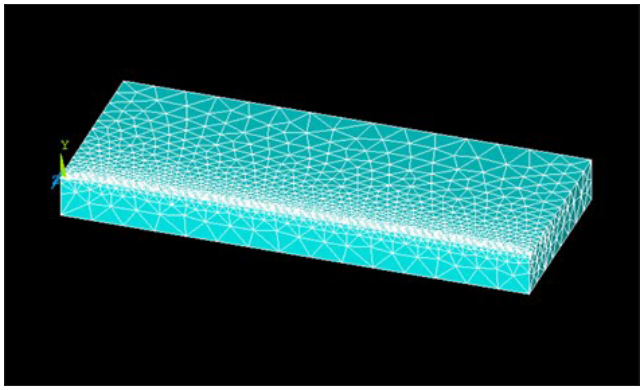

Figure 1: Tetrahedral meshed workpiece.

Numerical Model

Fourier's law for transient heat transfer analysis is taken for the calculation of the temperature profile and can be represented as Eq (1).

$$\frac{\partial}{\partial x}\left(K(T)\frac{\partial T}{\partial x}\right)+\frac{\partial}{\partial y}\left(K(T)\frac{\partial T}{\partial y}\right)+\frac{\partial}{\partial z}\left(K(T)\frac{\partial T}{\partial z}\right)+Q_v=\rho(T)c(T)\frac{\partial T}{\partial t} \quad (1)$$

Where, Q_v (W/m^3) is the rate of internally generated heat, t represents time; ρ (T) represents density of the material, c (T) and k (T) represent specific heat capacity and thermal conductivity, respectively which are temperature dependent.

Heat source models for HLAW

The combination of arc and laser heat sources give the net heat input for HLAW. The Gaussian heat source model is considered for distribution of heat obtained from arc welding and can be represented by using following mathematical Eq (2) and Eq (3).

$$q(r)=q_{\max}\exp(-3\frac{r^2}{R^2}) \quad (2)$$

$$q_{\max}=\frac{3}{\pi R^2}(Q) \quad (3)$$

Where, q(r) (W/m_2) is surface flux at radius r, R is the region where maximum percentage of heat flux is deposited, r (mm) is radial distance from center of the heat source, q_{max} (J) is the maximum heat input where Q = U × I × η, in which Q, U, I and η are heat input, arc voltage, arc current and arc thermal efficiency, respectively.

The Gaussian heat flux distribution is considered for laser beam and can be represented by using following mathematical Eq (4) and Eq (5).

$$Q(x,y)=q'_{\max}\exp\left(-2\frac{r'^2}{r_o^2}\right) \quad (4)$$

$$q'_{\max}=\frac{2AP}{\pi r_o^2} \quad (5)$$

Where, $q`$ (W/m^2) is the largest heat input at the center of heat source, r_0 which is equal to 1.5 x 10^{-4} m, is radius of laser beam, A is absorptivity of workpiece, P (W) is average LP of material and r'(m) is radial distance from the center of the heat source.

Boundary conditions

At the initial condition when time t = 0 sec, the T = T_∞ where, T_∞ (27 °C) is ambient temperature.

Convection heat loss

The heat dissipation through convection from the upper and lateral surfaces of workpiece (convection heat loss) is represented by Eq (6).

$$q_{conv}=h_{conv}(T-T_\infty) \quad (6)$$

Where, h_{conv} (10 $W/m^{2\circ}C$) is convective heat transfer coefficient and T is the surface temperature.

Radiation heat loss

The heat dissipation through radiation from the upper and lateral surfaces of the of workpiece (radiation heat loss) is represented by Eq (7).

$$q_{rad}=\varepsilon\sigma(T^4-T_\infty^4) \quad (7)$$

Where, ε is the emissivity (for steel it is assumed as 1), σ is the Stefan-Boltzmann constant (5.67 x 10^{-8} $W/m^{2\circ}C^4$).

Welding parameters

In the present work thermal gradient and thermal stresses are calculated at different LP, different arc power. Thermal analysis is also done on different WS keeping another parameter constant. Three cases have been taken in HLAW for analysis process as shown in table 4. A Nd:YAG laser (continuous wave) of 3 kW is considered with 1.5 × 10^{-4} m laser beam radius. Arc thermal efficiency was 0.7 and the region in

Table 4: Welding process parameters.

Case	LP (W)	Arc voltage (V)	Arc current (Amp)	WS (mm/min)
Case 1	150	20	160	600
Case 2	200	20	160	600
Case 3	150	30	300	600

which maximum percentage of the heat flux was deposited (R) was taken as 0.007 m. The absorptivity of material (A) was taken as 0.34.

Results and Discussion

Thermal analysis

For case 1 the maximum temperature was 2902.93 °C at the time of 4 sec. Temperature distribution at the end of HLAW for case 1 is shown in figure 2a. In case 2 where the LP is increased from 150 W to 200 W, the maximum temperature was recorded as 3830.01 °C at the time of 4 sec. Here, as the LP increases the heat input in the material increases and the result of which the maximum temperature of material increases. Temperature contour plot for case 2 is shown in figure 2b. In case 3 due to the increase in arc power i.e., arc voltage from 20 V to 30 V and arc current from 160 A to 300 A (keeping all other parameters same as in case 1) the maximum temperature of the material was recorded as 2912.37 °C at time 4 sec. Here the maximum temperature is greater than that of case 1 but lower than that of case 2. Temperature contour plot of this case 3 is shown in figure 2c.

Temperature distribution at LP of 150 W, arc power of 3200 W and WS of 600 mm/min at the time 1 sec (case 1) is shown in figure 3a. In this case the maximum temperature was 3111.71 °C. Figure 3b shows temperature distribution at WS of 900 mm/min (keeping all the parameter same as in case 1) at the time 1 sec and the maximum temperature of 3092.83 °C was noted in the workpiece. From the result it is clear that as we increase the WS of HLAW process the maximum temperature in the material decreases. The reason behind the decrease in temperature is interaction time because there is less amount of heat input in the material at the higher WS due to less interaction time.

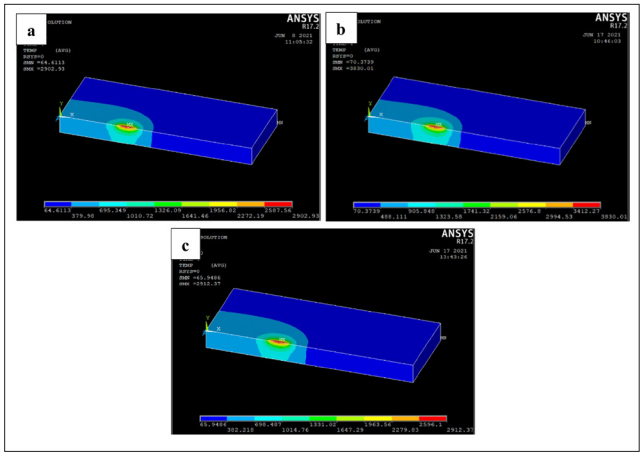

Figure 2: Temperature distribution in HLAW for (**a**) case 1, (**b**) case 2, and (**c**) case 3.

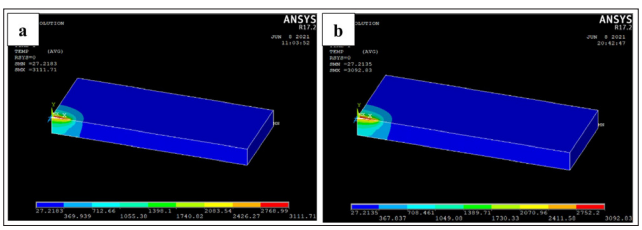

Figure 3: Temperature distribution at LP of 150 W, arc power of 3200 W and WS of (**a**) 600 mm/min and (**b**) 900 mm/min.

Residual stress analysis

The temperature histories obtained by the thermal analysis were served as thermal loads in the mechanical analysis. All the procedures used in thermal analysis is also used in mechanical analysis only boundary conditions and element type used in mechanical analysis is different. According to the model geometry of the welding process, largest stresses are expected parallel to the longitudinal direction. The contour plot for the longitudinal stress for all three cases is shown in figure 4. The maximum longitudinal stress in HLAW for case 1 was tensile in nature with magnitude of 122 MPa after 4 sec and its distribution was parallel to the welding direction and away from the weld center line as shown in figure 4a. Whereas for the case 2 the maximum longitudinal stress was tensile in nature with magnitude of 168 MPa after 4 sec (Figure 4b) which was higher than the longitudinal stress value obtained in case 1. The maximum longitudinal stress value for case 3 was also tensile in nature with magnitude of 122 MPa at 4 sec as shown in figure 4c which is somewhat equal to that of case 1 but lower than that of case 2. The nature of longitudinal stresses varies from compressive (yellowish color) to tensile (red color) as shown in contour plots (Figure 4).

The distribution of normal stress is along the thickness direction whose maximum value is 73.6 MPa after 4 second as shown is figure 5a for the case 1. The maximum value of normal stress for case 2 (Figure 5b) is 53.2 MPa which is lower than the normal stress value obtained in case 1. Whereas the maximum value of normal stress for case 3 (Figure 5c) is 71.7 MPa at 4 sec which is greater than the maximum value of normal stress obtained in case 2 but lower than the maximum value of normal stress obtained in case 1. The nature of normal stresses varies from compressive (yellowish color) to tensile (red color) as shown in contour plots (Figure 5).

Conclusions

The present work represents numerical assessment of hybrid laser-arc welding of NV E690 steel to predict the thermal profile and thermal stresses in the weldment. From simu-

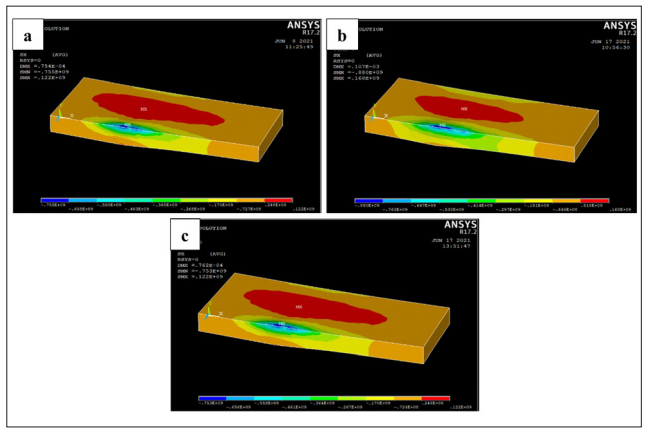

Figure 4: Longitudinal stress for **(a)** case 1, **(b)** case 2, and **(c)** case 3.

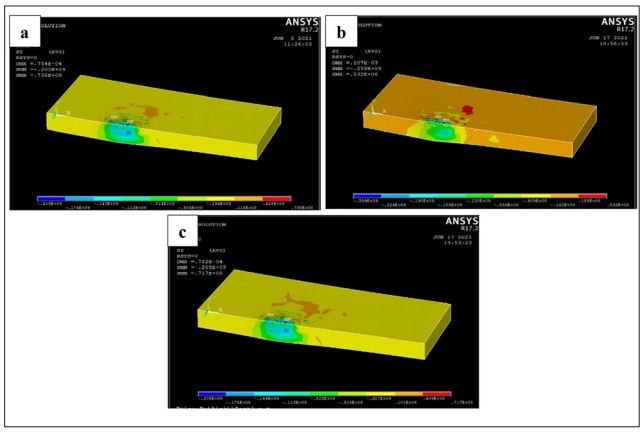

Figure 5: Normal stress for **(a)** case 1, **(b)** case 2, and **(c)** case 3.

lation results following conclusions can be made:

- In present work results obtained in case 1 and case 3 are almost similar. Increasing laser beam power causes an increase in the maximum temperature and maximizes the longitudinal residual stress in the weldment.
- An increase in welding speed can successfully reduce the peak temperature because during the process the higher the welding speed, the lower will be the heat input due to lower interaction time.
- The result obtained by simulation showed that the longitudinal stresses on the weldment surface were very high and the peak longitudinal tensile stresses which is tensile in nature were located near and around the heat affected zone.
- An increase in laser power decreases the normal stress and increase in arc power also decreases the normal stress but its magnitude is more than the value of the previous process.

Acknowledgements

None.

Conflict of Interest

There is no conflict of interest to this work.

Credit Author Statement

Alok Kumar: Simulation, Data collection, Analysis; Umesh Kumar Singh: Conceptualization, Design; Avanish Kumar Dubey: Conceptualization, Design; Pratiksha: Manuscript - original draft preparation, Writing - review and editing. All the authors read and approved the manuscript.

References

1. Acherjee B. 2018. Hybrid laser arc welding: state-of-art review. *Opt Laser Technol* 99: 60-71. https://doi.org/10.1016/j.optlastec.2017.09.038
2. Reisgen U, Olschok S, Jakobs S, Schleser M, Mokrov O, et al. 2012. Laser beam submerged arc hybrid welding. *Phys Procedia* 39: 75-83. https://doi.org/10.1016/j.phpro.2012.10.016
3. Sun GF, Wang ZD, Lu Y, Zhou R, Ni ZH, et al. 2018. Numerical and experimental investigation of thermal field and residual stress in laser-MIG hybrid welded NV E690 steel plates. *J Manuf Process* 34: 106-120. https://doi.org/10.1016/j.jmapro.2018.05.023
4. Yazdian N, Derakhshan ED, Kovacevic R. 2018. Numerical prediction and experimental analysis of the residual stress fields and generated distortion in hybrid laser/arc welded thick plates of high-strength steels. *Int J Adv Manuf Technol* 98: 2725-2735. https://doi.org/10.1007/s00170-018-2404-0
5. Xu G, Pan H, Liu P, Li P, Hu Q, et al. 2018. Finite element analysis of residual stress in hybrid laser-arc welding for butt joint of 12 mm-thick steel plate. *Weld World* 62: 289-300. https://doi.org/10.1007/s40194-017-0545-7
6. Zhan X, Li Y, Ou W, Yu F, Chen J, et al. 2016. Comparison between hybrid laser-MIG welding and MIG welding for the invar36 alloy. *Opt Laser Technol* 85: 75-84. https://doi.org/10.1016/j.optlastec.2016.06.001
7. Derakhshan ED, Yazdian N, Craft B, Smith S, Kovacevic R. 2018. Numerical simulation and experimental validation of residual stress and welding distortion induced by laser-based welding processes of thin structural steel plates in butt joint configuration. *Opt Laser Technol* 104: 170-182. https://doi.org/10.1016/j.optlastec.2018.02.026
8. Kong F, Ma J, Kovacevic R. 2011. Numerical and experimental study of thermally induced residual stress in the hybrid laser–GMA welding process. *J Mater Process Technol* 211(6): 1102-1111. https://doi.org/10.1016/j.jmatprotec.2011.01.012
9. Vishwakarma R, Singh U, Dubey A. 2022. Thermal analysis of laser-assisted friction stir welding (LAFSW) for different geometrical parameters. *Int J Laser Sci* 3: 65-87.
10. Singh UK, Dubey AK, Pandey A. 2021. Thermal analysis of friction stir welding for different tool geometries. In Singari RM, Mathiyazhagan K, Kumar H (eds) Advances in Manufacturing and Industrial Engineering: Select Proceedings of ICAPIE 2019. Springer, Singapore, pp 361-370.